

## Atomic structure of Si and Ge surfaces: Models for (113), (115), and stepped (001) vicinal surfaces

W. Ranke

*Fritz-Haber-Institut der Max-Planck-Gesellschaft, Faradayweg 4-6, D-1000 Berlin 33, West Germany*

(Received 14 August 1989)

A new class of structure models for the (113) and (115) orientations of Si and Ge is proposed. They are based on dimer and adatom formation as the main building blocks for the reduction of dangling bonds (DB), on relaxation towards more  $sp^2$ - or  $s^2p^3$ -like configurations, and on the minimization of strain. Four structural alternatives are discussed for (113) which are consistent with the observed  $3 \times 1$  and  $3 \times 2$  periodicities. They have either a low DB density and large strain or a higher DB density and low strain. For Si(113), a decision between them on the basis of the available experimental results is not unique. The analysis of the orientation-dependent adsorption of  $H_2S$  and  $NO$  in terms of preferential adsorption by certain structural elements favors the models for Ge(113) which have not the minimum DB density but the minimum of strain. Steps on (001) vicinals induce strain due to bond stretching which is equilibrated over the terraces as long as they are wide enough. The switching of the twofold periodicity of the dimers along  $[\bar{1}10]$  on (001) and its vicinals to the threefold periodicity at (115) is explained to occur because the  $3 \times n$  models resolve bond stretching into bond bending by a meandering arrangement of microterraces which are separated by the energetically most favorable type- $S_A$  single-layer steps.

### I. INTRODUCTION

After a large number of publications on the structure of low-Miller-index surfaces of Si and Ge, the basic mechanisms for their stabilization by reconstruction and relaxation seem to be established. In agreement with the first scanning tunneling microscopy (STM) image of the Si(111)-(7 $\times$ 7) surface by Binnig *et al.*,<sup>1</sup> the dimer-adatom-stacking-fault (DAS) model was put forward by Takayanagi *et al.*<sup>2</sup> The  $\pi$ -bonded chain model for Si(111)-(2 $\times$ 1), proposed by Pandey,<sup>3</sup> was confirmed by STM.<sup>4</sup> On Si(001) and Ge(001), the surface-atom dimerization, originally proposed by Chadi,<sup>5</sup> was confirmed by STM as well.<sup>6,7</sup> Many details like the asymmetry of the dimers on singular<sup>7</sup> and stepped Ge(001) (Ref. 8) and for Si(001) near defects<sup>6</sup> or steps<sup>8,9</sup> were observed, confirming the prediction<sup>5,10</sup> that rehybridization of surface atoms towards an ideally planar  $sp^2$  or an ideally rectangular  $s^2p^3$  configuration may reduce the surface energy. However, this tendency is less pronounced than on III-V compounds.

Very recently, also atomic steps on vicinal Si(001) (Refs. 8 and 9) and Ge(001) (Ref. 8) in the  $[\bar{1}10]$  zone were investigated by STM. The clear tendency of double step formation which was concluded before from low-energy electron diffraction (LEED)<sup>11-13</sup> was confirmed in agreement with calculations of step formation energies,<sup>14,15</sup> at least for not too wide terraces. A detail of the structure of the step riser, as predicted by Chadi<sup>15</sup> and confirmed experimentally,<sup>8,9</sup> is that it is made very smooth by adding a row of "rebonded" atoms in the lower ledge similar to the adatoms on Si(111)-(7 $\times$ 7). Each of these atoms saturates three dangling bonds (DB) while forming only one new one. However, the bond length is extended<sup>15</sup> which introduces considerable strain along the surface. Obviously, this strain is relieved across

the terraces by a corresponding relaxation of the surface dimers. If, however, the terraces become too narrow, the strain per dimer becomes too high so that the whole structure becomes unstable.<sup>15</sup>

This range of stepped surfaces with narrow terraces has not yet been investigated in detail. It is known, however, that at (115), which in the truncated bulk picture consists of (001)-oriented terraces two atomic rows wide and a riser consisting of one (111)-oriented row, the twofold periodicity of the (001)-oriented terraces along  $[\bar{1}10]$ , the direction of the edges, is replaced by a threefold periodicity yielding a  $3 \times 1$  pattern in LEED both on Si (Ref. 16) and Ge.<sup>17</sup> In the truncated bulk picture, (113) consists of alternating single rows of (001) and (111) orientation. Applying the idea of rebonding, the surface could be formed by rebonded atoms only. However, considerable bond stretching would be necessary and the surface energy turns out to be unreasonably high.<sup>18</sup> Also the threefold periodicity along  $[\bar{1}10]$  which is observed as well<sup>16,17</sup> is not easily understandable in a rebonding model. In this context, it is interesting that Bartelt *et al.*,<sup>19</sup> applying a Monte Carlo type simulation for the annealing process, do not end with structures with threefold periodicity along  $[\bar{1}10]$  on Si(113). They suppose that the correct lowest-energy structure was not found, because its reconstruction is so complex that the starting model was too far from it. This is a hint that the equilibrium structure must be quite different from all models considered so far. Depending on preparation and annealing temperature, a  $3 \times 1$  or a  $3 \times 2$  pattern is observed on Si(113) by LEED.<sup>16,20,21</sup> Usually, a very clear  $3 \times 1$  pattern is observed after sputtering and annealing.<sup>20</sup> However, thorough investigations have shown that the  $3 \times 1$  surface which forms above  $\sim 900$  K converts to the  $3 \times 2$  surface above  $\sim 1050$  K, which seems to be the stable structure on the clean surface. It converts slowly back to

$3 \times 1$  when the surface is kept at 300 K for several hours.<sup>20</sup> Therefore it cannot be excluded that the  $3 \times 1$  structure is stabilized by adsorbates or small residual bulk contaminations like carbon. There exists a STM image of a Si(113) facet on a nominally (112)-oriented sample from Berghaus *et al.*<sup>22</sup> which consists of a coexisting small ( $3 \times 1$ ) and larger ( $3 \times 2$ ) domains. These observations indicate a similar surface energy of both structures. The STM image is reproduced in Fig. 3 below and will be an important input for the models proposed in this paper. Also on Ge(113), both  $3 \times 1$  (Ref. 17) and  $3 \times 2$  structures were observed. However, the  $3 \times 2$  structure is the stable phase at low temperature and forms after cooling to 130 K.<sup>21</sup>

All experimental and theoretical findings on Si and Ge surface structures suggest the following principles to be important (listed approximately according to their significance): (1) Maximum of one DB per surface atom, (2) reduction of DB density by dimerization on square units of DB configurations like on (001) or by adatoms over three adjacent DB's similar to the adatoms on Si(111)-(7 $\times$ 7), (3) bond stretch by more than about 5% induces too much strain and is unfavorable, (4) bond angle deviations (bond bending) away from the directions in  $sp^3$ -hybridized atoms are "softer" than bond stretch, (5) rehybridization from  $sp^3$  towards  $sp^2$  or  $s^2p^3$  as observed in asymmetric dimers may stabilize structures, and (6)  $\pi$  bonding may significantly stabilize arrangements with almost parallel DB's on nearest-neighbor atoms.

Microscopic smoothness is not an important argument for the stability of a structure as is demonstrated by the Si(111)-(7 $\times$ 7) structure which is "rough" over three atomic layers.

This paper presents structure models for (113) and (115) surfaces of Si and Ge which behave similarly in this orientation range. The proposed structures combine the above principles and are consistent with existing STM images and the observed easy conversion of  $3 \times 1$  into  $3 \times 2$  periodicity on (113). They are based on a small number of building blocks for all orientations and explain the transition of twofold to threefold periodicity along  $[\bar{1}10]$  between (001) and (115) as being due to strain relief. In detail, however, the models are qualitative and need refinements using both experimental and theoretical methods.

In the next two paragraphs, possible structure models for (113) are presented and compared to existing experimental results. In Sec. II C models for (115) are proposed, based on the same ideas as for (113). The transition to stepped (001) vicinals is discussed in Sec. II D. After that, Sec. II E summarizes the concentrations of structural elements for (113), (115), (117), etc., and double-stepped (001) vicinals. They are compared to the orientation dependence of gas adsorption. The structure elements active for adsorption of different gases are extracted.

## II. RESULTS AND DISCUSSION

### A. Models for the (113) surfaces of Si and Ge

Side view and top view of the truncated bulk structure of the (113) surface are shown in Figs. 1(a), and 1(b). Two

types of atomic rows exist, one with two dangling bonds per atom as on (001) and one with one DB per atom as on (111). If every third atom in the rows with two DB's is shifted, as indicated in Fig. 1(b), dimers may be formed. The resulting structure [Fig. 1(c)] has a  $3 \times 1$  periodicity with a considerably reduced number of DB's (two per shifted atom). I call this structure  $3 \times 1$ , model 1, or simply  $(3 \times 1)$ -1. The structure has deep holes between the formed dimers, each surrounded by six atoms with one DB each. The structure may be stabilized by relaxation of these atoms into the direction schematically indicated for one hole by arrows. In this way, the strain imposed by the dimer formation may be reduced making them even more stable than on (001) and the relaxing atoms may assume a configuration nearer to  $sp^2$ .

In Fig. 1(d), units of five atoms are introduced into the holes of every second row of holes. These five-atom units can saturate the six DB's surrounding the hole and form only four new DB's. However, their introduction also costs energy because the relaxation of the former DB atoms has to be removed which introduces strain. One of the atoms of the former dimers between the five-atom units in the  $[3\bar{3}\bar{2}]$  direction is now fourfold coordinated and the other one [dotted in Fig. 1(d)] has a configuration which I denote as adatomlike (*A*). In a stick-and-ball model as shown in Fig. 2(a), its bond lengths have to be

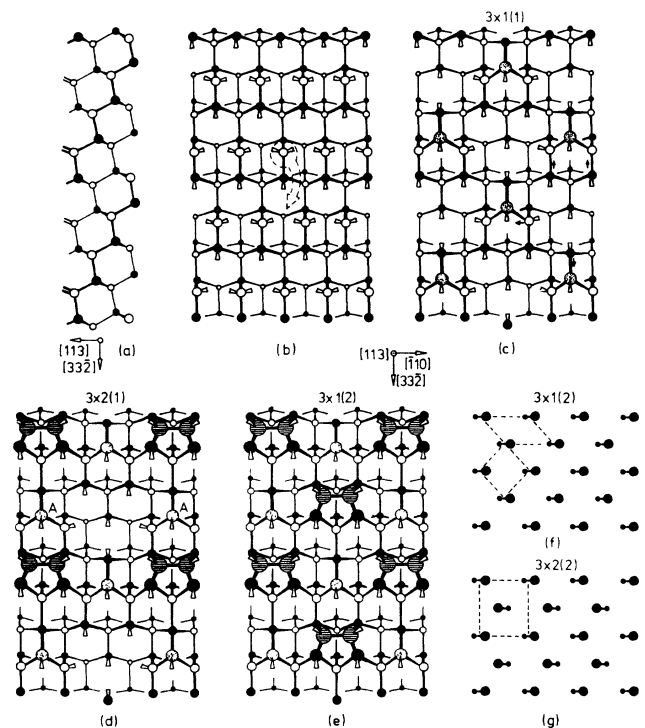


FIG. 1. Structure models of the (113) surface. The atoms of the two substrate sublattices are distinguished by solid and open circles. Dangling bonds are indicated. (a) Side view and (b) top view of the truncated bulk structure; (c)  $(3 \times 1)$ -1 model; (d)  $(3 \times 2)$ -1 model; (e)  $(3 \times 1)$ -2 model. If the top layer dimers (hatched) are asymmetric and tilted all into the same direction, a  $3 \times 1$  structure is preserved as schematically shown in (f). Alternating tilt directions yield a  $3 \times 2$  structure (g).

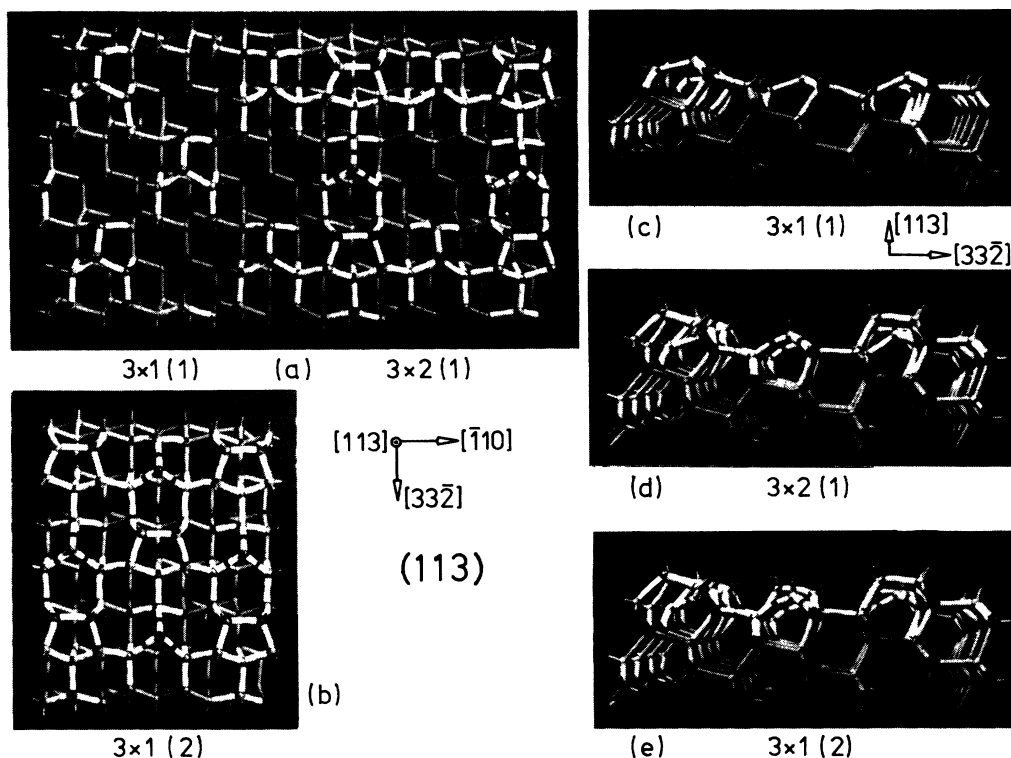


FIG. 2. Stick-and-ball models of the (113) surface. The bonds of surface atoms were formed using flexible sticks allowing for bond bending. The tetrahedral bond directions of the atoms are retained, however. The bonds marked with a black ring, associated with "adatoms," are extended by 10%. (a) Top view of  $(3 \times 1)$ -1 (left) and  $(3 \times 2)$ -1 (right); (b) top view of  $(3 \times 1)$ -2; (c)–(e): side views of  $(3 \times 1)$ -1,  $(3 \times 2)$ -1, and  $(3 \times 1)$ -2.

stretched by 5–10% to establish a stable model. The resulting structure has  $3 \times 2$  periodicity. I call it  $3 \times 2$ , model 1, or simply  $(3 \times 2)$ -1.

If also the remaining holes are filled with five-atom units, the  $3 \times 1$ , model-2 unit cell is formed as shown in Figs. 1(e) and 2(b). This surface has the lowest concentration of DB's, but, of course, also the highest concentration of adatoms with stretched bonds.

In general, one can expect that the top layer dimers [hatched in Figs. 1(d) and 1(e)] are not symmetric. As in the case of the (001) surface, a varying tilt direction of the dimers can introduce other periodicities.<sup>23,24</sup> The structure of Fig. 1(e) would retain a  $3 \times 1$  periodicity if all dimers were tilted into the same direction as schematically shown in Fig. 1(f) (only dimers shown). If the dimers of adjacent horizontal rows were tilted in opposite directions as in Fig. 1(g), a  $3 \times 2$  periodicity would result. This model will be called  $(3 \times 2)$ -2.

The dimers in Figs. 1(c), 1(d), and 1(e) are not all equivalent. The dotted atoms in Fig. 1(c) are bound to only threefold coordinated atoms. They, and as a consequence also the dimer, may therefore relax towards more  $sp^2$ - and  $s^2p^3$ -like configurations than is possible for dimers on (001). Also the hatched dimers in Figs. 1(d) and 1(e) are not "(001)-like." Both atoms are bound to one threefold coordinated atom each, very similar to dimers along double layer steps on (001) vicinals (see below). The dimers with dotted atom in Fig. 1(d) which lie be-

tween two five-atom units in the  $[\bar{1}10]$  direction have become (001)-like because, compared to Fig. 1(c), they are now bound only to fourfold coordinated atoms.

The densities of structural elements [total number of dangling bonds, (001)-like and other dimers, adatoms, other dangling bonds] for the presented (113) models are included in Table I.

### B. Experimental support for the proposed models

Strong support for the structures  $(3 \times 1)$ -1 and  $(3 \times 2)$ -1 comes from a STM image of Berghaus *et al.*,<sup>22</sup> a part of which is reproduced in Fig. 3(a). The image is taken from a (113) facet on a nominally (112)-oriented Si surface. It contains areas with  $3 \times 1$  and with  $3 \times 2$  periodicity. The transition from  $3 \times 1$  to  $3 \times 2$  areas occurs by filling the dark holes of every second horizontal row by which a hill is formed at these positions. This corresponds exactly to the relation between the models  $(3 \times 1)$ -1 and  $(3 \times 2)$ -1. Figure 3(b) presents a model containing both structures which reproduces very well the portion marked in Fig. 3(a).

The coexistence of  $3 \times 1$  and  $3 \times 2$  features in the STM image [Fig. 3(a)] is an indication that both structures are similar in energy. This would mean that the energy decrease by reduction of DB concentration by the five-atom units is almost canceled by the simultaneous introduction of strain as discussed in the preceding section.

TABLE I. Unit cell data and structural elements for all discussed structure models. The unit cell areas in the second column are given as multiples of the (001) unreconstructed unit cell area which is  $14.75 \times 10^{-16} \text{ cm}^2$  for Si and  $16.0 \times 10^{-16} \text{ cm}^2$  for Ge. Also the densities of structural elements are referred to the (001) unreconstructed unit cell areas. The absolute numbers per reconstructed surface unit cell are additionally given in brackets. Dimers bound to fully coordinated substrate atoms are (001)-like. "Other dimers" are those bound in part to substrate atoms with a dangling bond. Adatoms are atoms far away from lattice sites which saturate three dangling bonds of the substrate. "Other dangling bonds" are those not connected with dimers or adatoms.

| Orientation,<br>Unit cell              | Model<br>Unit cell<br>area | Inclination<br>from (001) | DB<br>(total) | Density and absolute number of structural elements |              |              |              |
|--|----------------------------|---------------------------|---------------|--|--------------|--------------|--------------|
|  |                            |                           |               | Dimers   |              | Adatoms      | Other DB     |
|  |                            |                           |               | (001)-like   | Others       |              |              |
| (001) $2 \times 1$                     | 2.0                        | 0                         | 1.0<br>(2)    | 0.5<br>(1)   | 0<br>(0)     | 0<br>(0)     | 0<br>(0)     |
| (111) $2 \times 1$ (S)<br>with adatoms | 11.08                      | 7.33°                     | 0.902<br>(10) | 0.361<br>(4)                                       | 0<br>(0)     | 0.180<br>(2) | 0<br>(0)     |
| Without adatoms                        | 11.08                      |                           | 1.083<br>(12) | 0.361<br>(4)                                       | 0.090<br>(1) | 0<br>(0)     | 0.181<br>(2) |
| (119) $2 \times 1$ (S)<br>with adatoms | 9.10                       | 8.93°                     | 0.878<br>(8)  | 0.329<br>(3)                                       | 0<br>(0)     | 0.220<br>(2) | 0<br>(0)     |
| Without adatoms                        | 9.10                       |                           | 1.098<br>(10) | 0.329<br>(3)                                       | 0.110<br>(1) | 0<br>(0)     | 0.220<br>(2) |
| $3 \times 1$                           | 13.65                      |                           | 1.098<br>(15) | 0.366<br>(5)                                       | 0.073<br>(1) | 0<br>(0)     | 0.220<br>(3) |
| (117) $2 \times 1$ (S)<br>with adatoms | 7.14                       | 11.42°                    | 0.841<br>(6)  | 0.280<br>(2)                                       | 0<br>(0)     | 0.280<br>(2) | 0<br>(0)     |
| Without adatoms                        | 7.14                       |                           | 1.121<br>(8)  | 0.280<br>(2)                                       | 0.140<br>(1) | 0<br>(0)     | 0.280<br>(2) |
| $3 \times 1$                           | 10.71                      |                           | 1.028<br>(11) | 0.280<br>(3)                                       | 0.093<br>(1) | 0.093<br>(1) | 0.187<br>(2) |
| (115)-(3×1)-1                          | 7.79                       | 15.79°                    | 1.155<br>(9)  | 0.257<br>(2)                                       | 0.128<br>(1) | 0<br>(0)     | 0.385<br>(3) |
| -(3×1)-2                               | 7.79                       |                           | 1.155<br>(9)  | 0.128<br>(1)                                       | 0.128<br>(1) | 0.128<br>(1) | 0.513<br>(4) |
| (113)-(3×1)-1                          | 4.98                       | 25.24°                    | 1.408<br>(7)  | 0<br>(0)   | 0.201<br>(1) | 0<br>(0)     | 1.006<br>(5) |
| -(3×2)-1                               | 9.95                       |                           | 1.207<br>(12) | 0.101<br>(1)                                       | 0.101<br>(1) | 0.101<br>(1) | 0.704<br>(7) |
| -(3×1)-2                               | 4.98                       |                           | 1.005<br>(5)  | 0<br>(0)   | 0.201<br>(1) | 0.201<br>(1) | 0.402<br>(2) |

Both  $(3 \times 1)-1$  and  $(3 \times 2)-1$  exhibit a considerable corrugation. The side views of both structures, seen in  $[\bar{1}10]$  direction, are shown in Figs. 2(c) and 2(d). Both structures look sawtoothlike with a corrugation amplitude and periodicity consistent with the TEM profile of Gibson *et al.*<sup>25</sup> Although Gibson *et al.* claim to have observed a onefold periodicity along  $[3\bar{3}\bar{2}]$ , a local twofold periodicity cannot be excluded, especially since the existence of antiphase domains shifted into  $[3\bar{3}\bar{2}]$  direction by one half of the periodicity length of the  $(3 \times 2)-1$  structure would produce profiles of seemingly onefold periodicity. Myler and Jacobi<sup>20</sup> have observed clearly different surface state bands for the Si(113)  $3 \times 1$  and  $3 \times 2$  structures, the latter exhibiting a surface state bond 0.9 eV below  $E_F$ . This is a position typical for DB-related surface states of dimers on Si(001).<sup>26</sup> It could be related with the top layer dimers of the five-atom units of  $(3 \times 2)-1$ . This surface state band is not observed on Si(113)- $(3 \times 1)$ . This is at least consistent with the strongly different structure of  $(3 \times 1)-1$ . There exist also dimers on this structure. However, as discussed in the preceding section, they are rotated by 90° and both atoms constituting the dimer are

bound in a different way to the substrate. They may thus be relaxed in a quite different way than the dimers on  $(3 \times 2)-1$ .

There exists, however, an experimental observation which would fit better with the alternative models  $(3 \times 1)-2$  and  $(3 \times 2)-2$ , i.e., the easy conversion of one periodicity into the other which was observed both for Si(113) (Refs. 17 and 20) and Ge(113) (Ref. 21) as described in the Introduction. Whereas such a conversion would need a considerable mass transport for the type-1 models, no mass transport but only a change of the dimer tilt direction for half the surface dimers would be necessary for the type-2 models. The TEM profile of Gibson *et al.*<sup>25</sup> would be consistent with the type-2 models as well [compare the side view, Fig. 2(e)]. Since the STM image of Berghaus *et al.*<sup>22</sup> was taken on a Si(113) facet on a macroscopically (112)-oriented surface, it could be possible that it does not represent the most stable surface structure. The electronic structure of both the type-2 models should be very similar, however, which is in contradiction to the results of Myler and Jacobi.

The situation is thus not yet clear, and it cannot be ex-

cluded that, depending on the precise preparation conditions, different models exist on the surface. If this is the case, all presented models should be quite similar in energy so that small distortions could shift the absolute energy minimum to another structure.

Although Si and Ge appear to behave generally similarly in the considered orientation range, it is, of course, quite possible that different models represent the global energy minimum on the two substrates.

### C. Model for the (115) surfaces of Si and Ge

To the author's knowledge the observation of  $3 \times 1$  periodicities in LEED both for Si(115) (Ref. 16) and Ge(115) (Ref. 17) is the only published experimental result concerning (115) structure. The same threefold periodicity along  $[\bar{1}10]$  as for (113) has encouraged me to

propose models based on the same structural elements as for (113).

Figure 4 shows these models. They are formed by introducing a second (001)-like dimer  $D2$  parallel to the single dimers  $D1$  of the (113) model  $(3 \times 1)-2$  [Fig. 1(e)]. If the former adatoms [dotted in Fig. 1(e)] are left on their place, they form now dimers of  $D3$  type in Fig. 4. At  $H$ , a hole is formed which has nearly the same shape as the holes in Figs. 1(c) and 1(d). It can, however, not be filled with a five-atom unit without breaking the dimer  $D2$  so that no reduction of the DB density would result. Actually, filling the holes with five-atom units would reproduce the same surface structure with only one small difference: The dimers of type  $D3$  would be replaced by an adatomlike configuration  $A$  as shown in the lower half of Fig. 4. Filling the space between four dimer pairs ( $D1$ ,

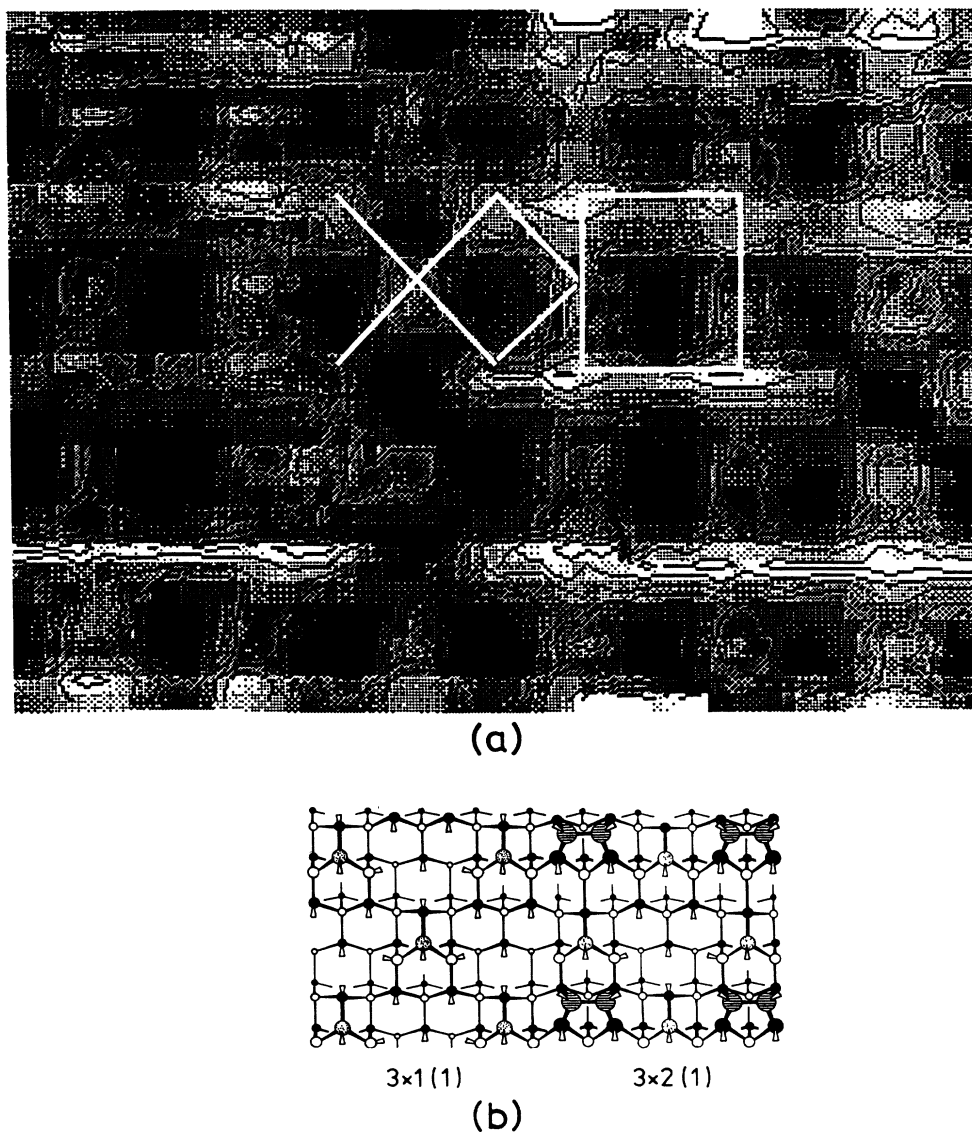


FIG. 3. (a) STM image of a (113) facet on a Si(112) surface, from Berghaus *et al.* (Ref. 22), displaying areas with  $3 \times 1$  (rhombic unit cell) and  $3 \times 2$  (rectangular unit cell) periodicity. The marked part of the image is modeled in (b) by the proposed  $(3 \times 1)-1$  and  $(3 \times 2)-1$  models. The same section is shown in Fig. 2(a) as stick-and-ball model.

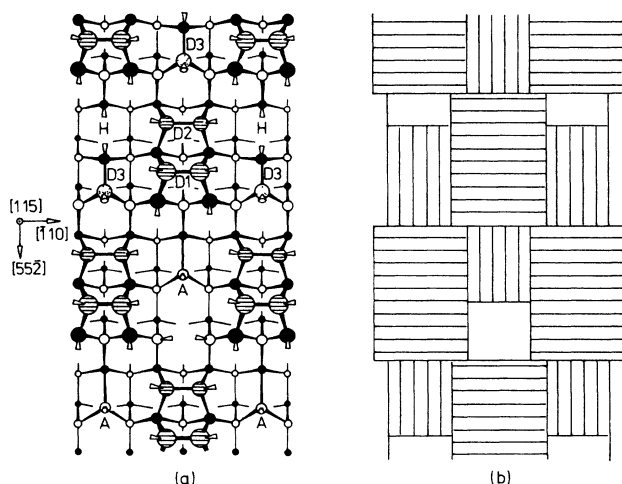


FIG. 4. (a) Model of  $(115) 3 \times 1$ . Upper half with a hole  $H$  and a dimer  $D3$  between four dimer pairs  $D1, D2$  [ $(3 \times 1)-1$ ]; lower half with adatoms  $A$  [ $(3 \times 1)-2$ ]; (b) same section as in (a), with the hatching direction giving the dimer direction, emphasizing the microterrace character of the structure.

$D2$ ) by a dimer  $D3$  or by an adatom  $A$  yields the same number of DB's. Both alternatives form a  $3 \times 1$  periodicity. The models with dimers of  $D3$  type and adatoms  $A$  are denoted as  $\text{Si}(115)-(3 \times 1)-1$  and  $\text{Si}(115)-(3 \times 1)-2$ , respectively.

#### D. Vicinals of (001) and transition to threefold periodicity

By introduction of further dimers parallel to  $D2$  in Fig. 4, corresponding structures for  $(117)$ ,  $(119)$ , etc. can be constructed with threefold periodicity along  $[\bar{1}10]$ . On the other hand, as described already in the Introduction, it is well established that vicinal faces with a macroscopic deviation of more than about  $1^\circ$  from  $(001)$  in the  $[\bar{1}10]$  zone form double layer steps with a twofold periodicity in the  $[\bar{1}10]$  direction. As on the singular  $(001)$  surface it is established by dimer rows on the terraces. Predicted by Chadi<sup>15</sup> and verified experimentally by Griffith *et al.*<sup>8</sup> and Wierenga *et al.*,<sup>9</sup> both Si and Ge show a row of rebonded atoms along the lower edge of the step with adatomlike configuration. These atoms reduce the density of DB's. At the same time, however, they introduce strain which can be relieved over the terraces, if they are not too narrow. When the terraces become too narrow, the adatom row becomes unstable. Chadi reports that this occurs already at  $(119)$  (Ref. 27) which corresponds to a terrace width of four  $(001)$  rows. My guess is that at the orientation where the adatom row becomes unstable, a transition to structures with threefold periodicities along  $[\bar{1}10]$  occurs. These structures have in common that the large  $(001)$  terraces are split into a meandering pattern of  $(001)$  microfacets, sometimes only one dimer large. The  $(115)$  structure in Fig. 4(a) is an example. The double layer steps are split into single layer steps. According to Chadi's nomenclature, these single layer steps are of the  $S_A$  type with the dimer axis on the upper terrace perpendicular to the edges. The energy per unit length of this

type of steps is the lowest of all possible models<sup>15</sup> so that the presented models are also in agreement with step energy considerations. The direction of the steps rotates by  $90^\circ$  from layer to layer. To emphasize the visibility of the microfacet arrangement, Fig. 4(b) shows them again with the hatching direction indicating the dimer direction of Fig. 4(a). This meandering dissolves the bond stretching into bond bending which costs less energy.

Experimentally, this transition region has not yet been investigated in detail. It could also be that it consists of a mixture of faceted of stepped  $(001)$  vicinals and a stable orientation with threefold periodicity as, e.g.,  $(115)$ .

#### E. Comparison of the structure models with adsorption measurements

The orientation dependence of the adsorption of gases has been investigated in our laboratory on cylindrical samples of Si, Ge, and GaAs.  $\text{H}_2\text{S}$  and NO show a very clear but distinctly different orientation-dependent adsorption behavior on Ge in the orientation range  $(001)$  to  $(113)$  considered in this paper. In this section I will analyze this behavior in terms of preferential adsorption ("titration") on certain structural elements of the structures discussed in the preceding sections.

The discussed structures are schematically compiled in Fig. 5. Only the dimers [(001)-like and others] and the adatoms are shown. For  $(115)$ , both dimer (model 1) and adatom (model 2) versions as discussed above are combined. For  $(117)$ , both the  $3 \times 1$  model and the stepped version with adatoms  $2 \times 1$  (S) are shown. If the adatom row were removed, another dimer in each row would form instead. Corresponding  $3 \times 1$  and stepped versions can be constructed for  $(119)$ ,  $(1111)$ , etc.

The structural data, concentrations, and absolute numbers per surface unit cell (in brackets) of the structural elements [(001)-like dimers, other dimers, adatoms, and other atoms with one DB each] for all discussed structures are listed in Table I.

In Fig. 6, the concentrations of structural elements are compared with the orientation-dependent amount of adsorbed species (solid dots) after exposure to  $\text{H}_2\text{S}$  [from Ref. 28, Fig. 6(a)] and NO [from Ref. 29, Fig. 6(b)]. After an exposure of 2 L  $\text{H}_2\text{S}$  at 300 K ( $1 \text{ L} = 1.33 \times 10^{-16}$  mbar s) in Fig. 6(a), the sulfur  $S_{KLL}$  Auger intensity decreases almost linearly between  $(001)$  and  $(113)$ . As discussed in Ref. 30,  $\text{H}_2\text{S}$  is adsorbed dissociatively at  $(001)$  in the form of  $\text{SH} + \text{H}$  in this fast adsorption step. A very similar linear decrease of the concentration of adsorbed OH and H between  $(001)$  and  $(113)$  is also observed after condensation of a thin water layer at 110 K and warming up to 300 K.<sup>30,31</sup>

The maximum at  $(001)$  and the monotonous decrease suggest that dimers are the responsible reaction and/or adsorption sites. This is tested by comparison with the orientation-dependent concentration of dimers from the models. For stepped models without adatoms, the total dimer concentration (crosses) does not decrease steeply enough. At  $(113)$ , the total dimer concentration is equal for all models (triangle), but also too high. For the stepped surfaces, the concentration of only the  $(001)$ -like

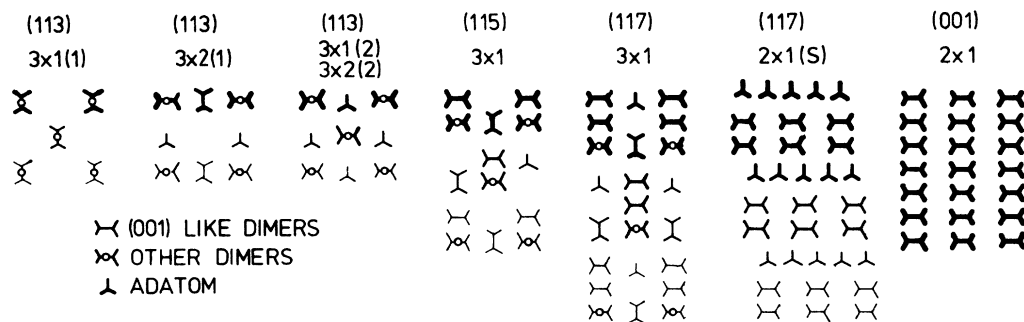


FIG. 5. Schematic representation of the structures discussed in this paper. Only surface dimers and adatoms are shown. For details see text.

dimers (squares), which is equal for models with and without adatoms, decreases as steeply as the measured data, however. Also at (115) and (113), the measured data fit better with the (001)-like dimer concentrations for the different models (circles). A decision between them is not possible, however, because the measured data lie between them. A mixture of domains with different structures cannot be excluded as well.

The result is that the proposed models are consistent with the assumption that the fast adsorption of  $H_2S$

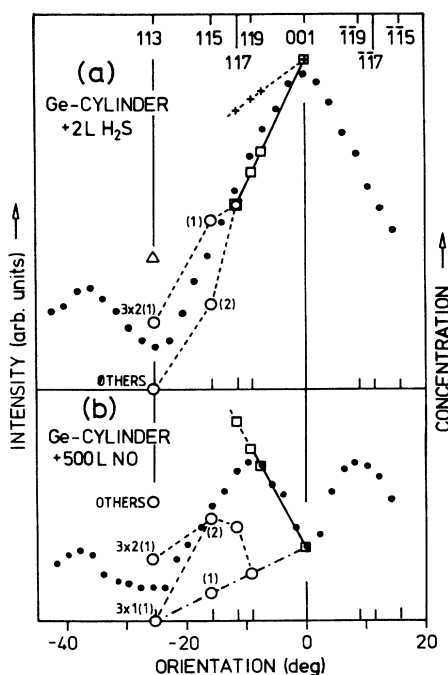


FIG. 6. Comparison of the orientation-dependent amount of adsorbed gases on a cylindrical Ge sample with the concentration of structural elements. (a) Solid dots: Auger S KLL intensity after 2 L  $H_2S$  at 300 K, from Ref. 28; +, all dimers, stepped models without adatoms;  $\Delta$ , all dimers on (113), all models;  $\square$ , (001)-like dimers, stepped models  $\circ$  (001)-like dimers,  $3 \times n$  models. (b) Solid dots: Auger O KLL intensity after 500 L NO at 300 K, from Ref. 29;  $\square$ , adatoms, stepped models with adatoms;  $\circ$ , adatoms,  $3 \times n$  models.

occurs at (001)-like dimers.

The orientation dependence of NO adsorption has quite different characteristics. NO is adsorbed dissociatively at 300 K,<sup>29</sup> the intensity ratio of N and O is equal for all orientations. Therefore Fig. 6(b) shows only the O KLL Auger intensities (solid dots). The linear increase of the adsorbed amount when deviating from (001) indicates a clear step influence. After a maximum at (119), the intensity decreases towards (113). Since adsorption at (001) is not zero, we have to assume that dimers also adsorb (and dissociate) NO. If we assume that only (001)-like dimers are responsible for this adsorption and that  $(3 \times 1)$ -1 [which has no (001)-like dimers] is the correct structure at (113), the dash-dotted line approximates the almost linear decrease of (001)-like dimers and the NO adsorption on them.

Two kinds of step-related sites could then be responsible for the additionally adsorbed species: adatoms or other dangling bonds not related with adatoms or dimers. For stepped models with adatoms, there exist no such other DB's. For stepped models without adatoms, their concentration is the same as for adatoms in the adatom models (squares) [fitted to the steep increase of measured points near (001)]. For (115) and (113), however, the concentration of other DB's is quite high for all models, actually so high that they would fall out of the frame of the figure.

The situation is quite different for adatoms. Their concentration on stepped models with adatoms is fitted to the measured data near (001) and fits them until near (119), where according to Chadi the adatom models should become unstable in the case of Si.<sup>27</sup> The (115)- $(3 \times 1)$ -2 model fits the data very well, and at (113) the data points lie between the values for  $(3 \times 1)$ -1 and  $(3 \times 2)$ -1. The models  $(3 \times 1)$ -2 and  $(3 \times 2)$ -2 do not fit. Between about (119) and (115), neither stepped models (squares) nor  $3 \times 1$  models [like circle at (117)] fit the data. A mixture of domains of stepped and  $3 \times 1$  areas is possible, but also a mixture of, e.g., (119) and (115) facets.

The dash-dotted baseline in Fig. 6(b) represents adsorption on (001)-like dimers only. If all dimers would adsorb, the baseline would not approach zero at (113) but would instead end almost at the position of the experimental data. Then no additional adsorption due to adatoms would be necessary at (113) which would favor the

( $3\times 1$ )-1 model. In LEED, a  $3\times 1$  pattern is observed so that ( $3\times 1$ )-1 seems the most probable structure of Ge(113).

As a result for Ge, the NO adsorption data are consistent with a slow adsorption on dimers and a fast adsorption on adatoms. At (115), model 2 with adatoms is favored. At (113), both  $\text{H}_2\text{S}$  and NO adsorption are consistent with ( $3\times 1$ )-1 and ( $3\times 2$ )-1. NO adsorption rules out the models ( $3\times 1$ )-2 and ( $3\times 2$ )-2. Since a  $3\times 1$  pattern is observed in LEED, the ( $3\times 1$ )-1 model is the only model consistent with all experimental data.

### III. SUMMARY

A new class of structure models for the reconstructed (113) and (115) surfaces of Si and Ge is presented. There do not yet exist conclusive experimental or theoretical facts which would prove that these models are correct and which of them is correct in case of presented alternative models. However, all facts known so far are consistent with them, giving them a high degree of probability of being correct. In particular, the models explain the observed threefold periodicity along  $[\bar{1}10]$ . They are consistent with a high resolution electron microscopic profile image of Si(113) and with adsorption measurements of  $\text{H}_2\text{S}$  and NO on Ge in the orientation range (001)-(115)-(113). The adsorption of these gases is sensitive to the local structure so that titration of the density of different sites is possible. On (113), both  $3\times 1$  and  $3\times 2$  structures exist. Two alternative models for each of them are proposed. One set of them, referred to as ( $3\times 1$ )-1 and ( $3\times 2$ )-1, is in excellent agreement with a

STM image of Si(113) which contains both  $3\times 1$  and  $3\times 2$  patches. The observed easy conversion of  $3\times 2$  into  $3\times 1$  on Si and  $3\times 1$  into  $3\times 2$  on Ge would, however, be in better agreement with the proposed alternative type-2 models because no mass transport would be necessary in this case. Since the balance between DB density and strain is crucial, it is possible that all proposed models exist in reality, depending on the precise conditions of preparation and cleanliness. The models are mainly based on structural elements which are known to exist on (001) and its vicinals, namely dimers and that kind of adatoms which form the "rebonded" row of atoms along double layer steps near (001). These rebonded adatoms induce considerable strain which destabilizes the stepped structures for narrow terraces. It is proposed that the observed change from stepped (001) vicinals with twofold periodicity along  $[\bar{1}10]$  to the structures observed at (115) and (113) with threefold periodicity is driven by strain minimization. Actually, the models for (115) and (113) can be considered as a meandering sequence of microterraces separated by the energetically most favorable single layer steps of  $S_A$  type which resolves the bond stretching strain into the "softer" bond bending.

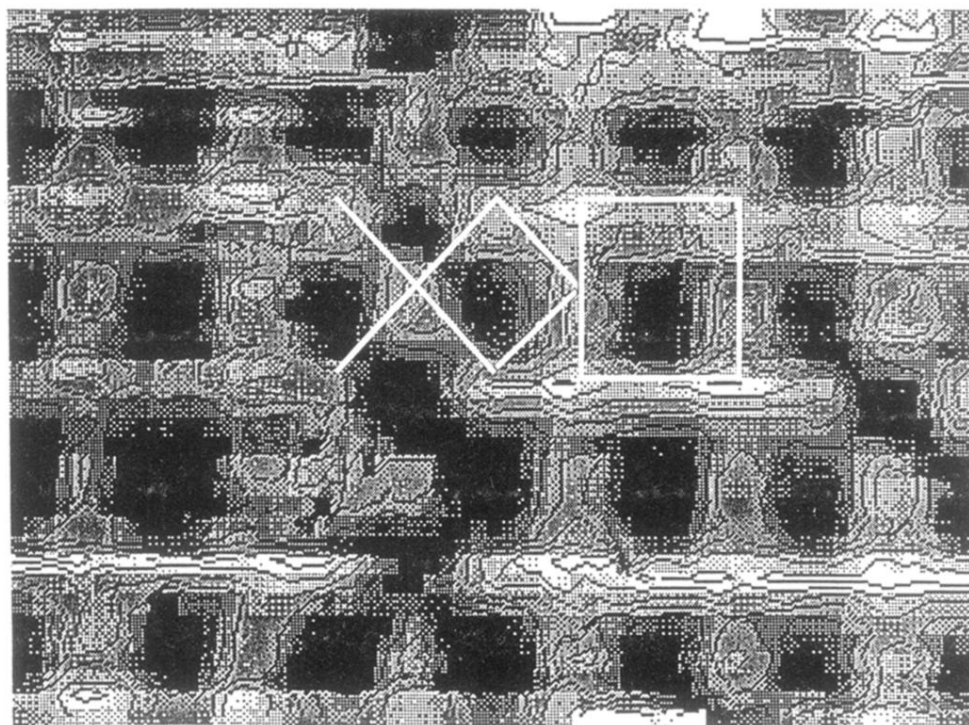
### ACKNOWLEDGMENTS

The author wants to thank D. J. Chadi for his encouragement to write this paper, K. Jacobi, U. Myler, and E. Schröder-Bergen for many helpful discussions, and H. Neddermeyer for making available the STM image of Si(113).

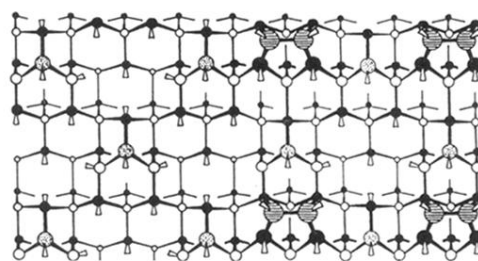
- 
- <sup>1</sup>G. Binnig, H. Rohrer, Ch. Gerber, and E. Weibel, *Phys. Rev. Lett.* **50**, 120 (1983).  
<sup>2</sup>K. Takayanagi, Y. Tanishiro, M. Takahashi, and S. Takahashi, *J. Vac. Sci. Technol. A* **3**, 1502 (1985).  
<sup>3</sup>K. C. Pandey, *Phys. Rev. Lett.* **47**, 1913 (1981); **49**, 223 (1982).  
<sup>4</sup>R. M. Feenstra, W. A. Thompson, and A. P. Fein, *Phys. Rev. Lett.* **56**, 608 (1986); *J. Vac. Sci. Technol. A* **4**, 1315 (1986).  
<sup>5</sup>D. J. Chadi, *Phys. Rev. Lett.* **43**, 43 (1979).  
<sup>6</sup>R. M. Tromp, P. J. Hamers, and J. E. Demuth, *Phys. Rev. Lett.* **55**, 1303 (1985); R. J. Hamers, R. M. Tromp, and J. E. Demuth, *Surf. Sci.* **181**, 346 (1987).  
<sup>7</sup>J. A. Kubby, J. E. Griffith, R. S. Becker, and J. S. Vickers, *Phys. Rev. B* **36**, 6079 (1987).  
<sup>8</sup>J. E. Griffith, J. A. Kubby, P. E. Wierenga, R. S. Becker, and J. S. Vickers, *J. Vac. Sci. Technol. A* **6**, 493 (1988).  
<sup>9</sup>P. E. Wierenga, J. A. Kubby, and J. E. Griffith, *Phys. Rev. Lett.* **59**, 2169 (1987).  
<sup>10</sup>F. Bechstedt and D. Reichardt, *Surf. Sci.* **202**, 83 (1988).  
<sup>11</sup>B. Z. Olshanetsky, S. M. Repinsky, and A. A. Shklyayev, *Surf. Sci.* **69**, 205 (1977).  
<sup>12</sup>B. Z. Olshanetsky and A. A. Shklyayev, *Surf. Sci.* **82**, 445 (1979).  
<sup>13</sup>R. Kaplan, *Surf. Sci.* **93**, 145 (1980).  
<sup>14</sup>D. E. Aspnes and J. Ihm, *Phys. Rev. Lett.* **57**, 3054 (1986).  
<sup>15</sup>D. J. Chadi, *Phys. Rev. Lett.* **59**, 1691 (1987).  
<sup>16</sup>B. Z. Olshanetsky and V. I. Mashanov, *Surf. Sci.* **111**, 414 (1981).  
<sup>17</sup>B. Z. Olshanetsky, V. I. Mashanov, and A. I. Nikiforov, *Surf. Sci.* **111**, 429 (1981).  
<sup>18</sup>D. J. Chadi, *Phys. Rev. B* **29**, 785 (1984).  
<sup>19</sup>N. C. Bartelt, E. D. Williams, R. J. Phaneuf, Y. Yang, and S. Das Sarma, *J. Vac. Sci. Technol. A* **7**, 1898 (1989).  
<sup>20</sup>U. Myler and K. Jacobi, *Surf. Sci.* **220**, 353 (1989).  
<sup>21</sup>W. Ranke (unpublished).  
<sup>22</sup>Th. Berghaus, St. Tosch, and H. Neddermeyer (private communication).  
<sup>23</sup>D. J. Chadi, *Appl. Opt.* **19**, 3971 (1980).  
<sup>24</sup>J. Ihm, D. H. Lee, J. D. Joannopoulos, and J. J. Xiong, *Phys. Rev. Lett.* **51**, 1872 (1983).  
<sup>25</sup>J. M. Gibson, M. L. McDonald, and F. C. Unterwald, *Phys. Rev. Lett.* **55**, 1765 (1985).  
<sup>26</sup>See, e.g., G. V. Hansson and R. I. G. Uhrberg, *Surf. Sci. Rep.* **9**, 197 (1988).  
<sup>27</sup>D. J. Chadi (private communication).  
<sup>28</sup>H. J. Kuhr, W. Ranke, and J. Finster, *Surf. Sci.* **178**, 171 (1986).  
<sup>29</sup>W. Ranke, X. H. Chen, and E. Schröder-Bergen, *Vacuum* (to be published).  
<sup>30</sup>H. J. Kuhr and W. Ranke, *Surf. Sci.* **189/190**, 420 (1987).  
<sup>31</sup>H. J. Kuhr and W. Ranke, *Surf. Sci.* **187**, 98 (1987).







(a)



$3 \times 1 (1)$

$3 \times 2 (1)$

(b)

FIG. 3. (a) STM image of a (113) facet on a Si(112) surface, from Berghaus *et al.* (Ref. 22), displaying areas with  $3 \times 1$  (rhombic unit cell) and  $3 \times 2$  (rectangular unit cell) periodicity. The marked part of the image is modeled in (b) by the proposed  $(3 \times 1)$ -1 and  $(3 \times 2)$ -1 models. The same section is shown in Fig. 2(a) as stick-and-ball model.